THE JOURNAL OF BIOLOGICAL CHEMISTRY VOL. 286, NO. 31, pp. 27825–27835, August 5, 2011

A Crucial Sequence for Transglutaminase Type 2 Extracellular Trafficking in Renal Tubular Epithelial Cells Lies in Its N-terminal β-Sandwich Domain[S]

Received for publication, January 28, 2011, and in revised form, June 5, 2011 Published, JBC Papers in Press, June 7, 2011, DOI 10.1074/jbc.M111.226340

Che-Yi Chou[‡§], Andrew J. Streets[‡], Philip F. Watson[¶], Linghong Huang[‡], Elisabetta A. M. Verderio[‖], and Timothy S. Johnson[‡1]

From the [‡]Academic Nephrology Unit (Sheffield Kidney Institute) and [¶]Department of Human Metabolism, University of Sheffield, Sheffield S10 2RZ, United Kingdom, [§]Institute and Division of Nephrology, Department of Internal Medicine, China Medical University Hospital, Taichung 40402, Taiwan, and [‖]Biomedical Life and Health Research Centre, School of Science and Technology, Nottingham Trent University, Nottingham NG11 8NS, United Kingdom

Transglutaminase type 2 (TG2) catalyzes the formation of an ε-(γ-glutamyl)-lysine isopeptide bond between adjacent peptides or proteins including those of the extracellular matrix (ECM). Elevated extracellular TG2 leads to accelerated ECM deposition and reduced clearance that underlie tissue scarring and fibrosis. The extracellular trafficking of TG2 is crucial to its role in ECM homeostasis; however, the mechanism by which TG2 escapes the cell is unknown as it has no signal leader peptide and therefore cannot be transported classically. Understanding TG2 transport may highlight novel mechanisms to interfere with the extracellular function of TG2 as isoform-specific TG2 inhibitors remain elusive. Mammalian expression vectors were constructed containing domain deletions of TG2. These were transfected into three kidney tubular epithelial cell lines, and TG2 export was assessed to identify critical domains. Point mutation was then used to highlight specific sequences within the domain required for TG2 export. The removal of β-sandwich domain prevented all TG2 export. Mutations of Asp[94] and Asp[97] within the N-terminal β-sandwich domain were identified as crucial for TG2 externalization. These form part of a previously identified fibronectin binding domain ([88]WTATVVDQQDCTLSLQLTT[106]). However, siRNA knockdown of fibronectin failed to affect TG2 export. The sequence [88]WTATVVDQQDCTLSLQLTT[106] within the β-sandwich domain of TG2 is critical to its export in tubular epithelial cell lines. The extracellular trafficking of TG2 is independent of fibronectin.

Elevated tissue transglutaminase (transglutaminase type 2 (TG2)[2]) activity is associated with abnormal wound healing (1). This includes liver (2), pulmonary (3), heart (4), and kidney fibrosis (5) as well as atherosclerosis (6). The process of scarring and fibrosis is linked to the increased synthesis of TG2 and most importantly increased export of TG2 to the interstitial space. Once outside the cell TG2 is able to cross-link extracellular matrix (ECM) proteins such as fibronectin and collagen (7) by the incorporation of an ε-(γ-glutamyl)-lysine dipeptide bond (8). Studies have shown that this can accelerate the deposition of available ECM components while at the same time confer resistance to proteolytic clearance by the matrix metalloproteinase system (9, 10). Taken together, this causes an accumulation of ECM proteins and thus scar tissue (9). Furthermore, TG2 has an emerging role in the activation of latent TGF-β1 in the scarring process (11) and has also been associated with interleukin-6 (12) and tumor necrosis factor-α activation pathways (13).

Inhibition of TG2 *in vitro* decreases extracellular matrix levels (14), and cells derived from TG2 knock-out mice have lower levels of mature ECM (9). *In vivo* application of TG2 inhibitors in models of chronic kidney disease reduces the development of glomerulosclerosis and tubulointerstitial fibrosis, preserving renal function (15, 16). Similar benefits are seen in the TG2 knock-out mouse subjected to unilateral ureteric obstruction (17).

The pathological role of TG2 in fibrosis is tightly associated with its trafficking to the extracellular environment (5, 10, 18) where it has both enzymatic (post-translational ECM modification and activation of cytokines (19, 20)) and non-enzymatic roles (cell migration, adhesion (21), and growth (1)). However, the mechanism by which TG2 is trafficked to the extracellular space remains unknown. The normal secretary pathway for proteins through the endoplasmic reticulum, Golgi apparatus, and plasma membrane to the extracellular environment (22) requires the protein to have a leader sequence. TG2 has no leader sequence; therefore, it cannot be exported via the Golgi apparatus (23, 24). Recent studies have highlighted several molecules such as fibroblast growth factor-1 and -2 (25) that like TG2 are exported without a leader sequence. Therefore, TG2 must be trafficked to the cell surface by an alternative (or unconventional) export mechanism. This mechanism would likely rely on specific motifs within the TG2 molecule that are essential to this process.

[S] The on-line version of this article (available at http://www.jbc.org) contains supplemental Figs. 1–3.

[1] To whom correspondence should be addressed: Academic Nephrology Unit (Sheffield Kidney Inst.), School of Medicine, University of Sheffield, Beech Hill Rd., Sheffield S10 2RZ, UK. Fax: 44-114-271-1711; E-mail: T.Johnson@Sheffield.ac.uk.

[2] The abbreviations used are: TG2, transglutaminase type 2 (tissue transglutaminase); ECM, extracellular matrix; TEC, tubular epithelial cell line; OK, opossum kidney; MDCK, Madin-Darby canine kidney; TG, transglutaminase; TRITC, tetramethylrhodamine isothiocyanate; ER, endoplasmic reticulum.

TABLE 1
Forward and reverse primers (5′ to 3′ for both) used to generate TG2 deletions and point mutations. The constructs are shown as three-dimensional schematics in supplemental Fig. 2

Construct		Forward primers	Reverse primers
tg		CACCATGGCCGAGGAGCTGGTCTT	AAATCCGCCCCGGTTACTACTGT
-bsw		CACCATGCTGTGTACCTGGACTCG	AAATCCGCCCCGGTTACTACTGT
-b2		CACCATGGCCGAGGAGCTGGTCTT	AAAGTAGAGGTCCCTCTCAGCCA
-b1b2		CACCATGGCCGAGGAGCTGGTCTT	AAAGTTCGCCCTTGTGAAGGCCT
-bwb2		CACCATGCTGTGTACCTGGACTCG	AAAGTAGAGGTCCCTCTCAGCCA
core		CACCATGCTGTGTACCTGGACTCG	AAAGTTCGCCCTTGTGAAGGCCT
f1	^{88}WTATVVAQQDCTLSLQLTT^{106}	CAGCCACCGTGGTGGCCCAGAAAGACTGCAC	GTGCAGTCTTGCTGGGCCACCACGGTGGCTG
f2	^{88}WTATVVDQQACTLSLQLTT^{106}	TGGTGGACCAGCAAGCCTGCACCCTCTCGCT	AGCGAGAGGGTGCAGGCTTGCTGGTCCACCA
f3	^{88}WTATVVAQQACTLSLQLTT^{106}	CAGCCACCGTGGTGGCCCAGCAAGCCTGCA CCCTCTCGCT	AGCGAGAGGGTGCAGGCTTGCTGGGCCACCA CGGTGGCTG

The aim of this study was to use deletion and point mutation studies to identify crucial elements within the TG2 molecule required for its export from renal tubular epithelial cells that may give an insight to the export pathway. This will provide new targets for TG2-specific interventional strategies in treating scarring and fibrosis.

MATERIALS AND METHODS

cDNA and Vectors—All constructs were prepared by PCR using the human TG2 cDNA as a template (26) using high fidelity *Pfu*Turbo polymerase (Stratagene). Primers for the domain deletion and point mutation constructs are shown in Table 1. PCR products were initially inserted in the pENTR Directional TOPO vector (Invitrogen) before transfer to the pcDNA™ 6.2/nTC-Tag-DEST tetracysteine tag vector (Invitrogen). The pFC14K CMV Flexi HaloTag vector and HaloTag® biotin ligand were obtained from Promega. The identity of all cDNA constructs was confirmed by DNA sequencing (Core Genomic Facility of the University of Sheffield) using a T7 promoter primer and thymidine kinase poly(A) reverse primer.

Cell Culture—OK cells (27) and rat NRK-52E tubular epithelial cells (28) were obtained from the European Cell Culture Collection. Canine MDCK II cells were a gift from N. Simmons (University of Newcastle, Newcastle, UK). All cells were grown in complete DMEM supplemented with 10% FBS, 100 units/ml penicillin, and 100 μg/ml streptomycin at 37 °C in 5% CO_2 atmosphere. To determine basolateral or apical TG2 trafficking, cells were grown in 6-well culture inserts (0.4-μm pores, transparent polyethylene terephthalate membrane, Falcon). The culture medium in the inserts represents apical TG2 secretion, and that outside the insert represents basolateral TG2 secretion.

Cell Transfection—Constructed cDNA were transfected in renal epithelial cells using Amaxa Nucleofector (Amaxa, Cologne, Germany). All transfections were performed using the Ingenio electroporation solution (Geneflow, Staffordshire, UK). Optimized programs were A20 for opossum proximal tubule cells (OK), L-05 for MDCK II, and X-01 for NRK-52E cells with 5 μg of selected vectors. This approach ensured that similar levels of transfected TG2 constructs were delivered to each cell line, and thus comparable increases in TG2 were seen in each cell line. The cells were grown in a 6-well plate post-transfection and incubated at 37 °C for 48 h before analysis. 5 μg of vector was selected for transfection as it produced TG2 levels within the linear range of TG2 assays (supplemental Fig. 1A) Stable transfectants were selected by blasticidin resistance (Invitrogen).

Preparation of Cell Lysates—Cells were trypsinized, centrifuged at 300 × *g* for 2 min, and homogenized by sonication in 100 μl of STE buffer (0.32 M sucrose, 5 mM Tris, 2 mM EDTA, pH 7.5) containing protease inhibitors (1 mM leupeptin, 1 mM benzamidine, and 1 mM phenylmethylsulfonyl fluoride (PMSF)).

Preparation of Conditioned Medium—48 h after transfection, medium was then replaced with 1 ml of serum-free medium. The medium was collected after 4-h incubation and centrifuged at 10,000 × *g*. The supernatant was used for analysis.

Total Transglutaminase Activity in Cell Lysate and Medium—Total TG2 activity was measured by the incorporation of biotinylated TVQQEL peptide (a unique TG2 substrate) into casein using a modified ELISA described by Trigwell *et al.* (29). 96-well plates were precoated with 1 mg/ml casein in 50 mM sodium carbonate, pH 7.5 and blocked with 250 μl of blocking solution (0.1% BSA in 50 mM sodium carbonate) at 37 °C for 1 h. The reaction was started by mixing 50 μl of cell lysates or medium with 150 μl of reaction buffer (13.3 mM dithiothreitol, 6.7 mM $CaCl_2$, 10 μM biotin-TVQQEL in 100 mM Tris-HCl, pH 8.5) at 37 °C for 1 h. 200 μl of diluted Extravidin-peroxidase (1:5000) in blocking solution were added and incubated for 1 h at 37 °C. The color was revealed with 200 μl of 3,3′,5,5′-tetramethylbenzidine solution. The color development was stopped with 50 μl of 2.5 M H_2SO_4. Absorbance was read at 450 nm in a Labsystems Multiskan Ascent plate reader using Genesis Software (version 3.05). The TG activity was calculated in units of TG activity from a TG2 *versus* absorbance at 450 nm standard curve (supplemental Fig. 1B) obtained from guinea pig liver transglutaminase (T006, Zedira).

Immunoblotting—The protein concentrations of cell lysates and medium were determined using the bicinchoninic acid (BCA) assay. Lysates (20 μg) or 20 μl of medium were diluted with reducing buffer, incubated in a boiling water bath for 5 min, electrophoresed on 5% (fibronectin) or 7.5% (TG2) SDS-polyacrylamide gels, transferred to nitrocellulose, and probed with either anti-TG2 (clone cub7402, ab2306, Abcam) or anti-fibronectin (ab6328, Abcam) antibody. β-Actin (Abcam) was used as a loading control. Antibody binding was revealed using

a polyclonal anti-mouse horseradish peroxidase-conjugated antibody (P0447, Dako) and developed using enhanced chemiluminescence (ECL) (BD Biosciences). For the measurements of TG2 in culture medium, the film was exposed for at least 1 h.

Assay of Extracellular Transglutaminase Activity—Extracellular TG activity was measured by the incorporation of biotinylated cadaverine into fibronectin as described previously (30). Briefly, cells were harvested after 48 h post-transfection using EDTA in PBS. 8×10^4 cells were resuspended in 100 μl of serum-free DMEM containing 0.1 mM biotinylated cadaverine (Molecular Probes) and placed into a 96-well plate precoated with fibronectin at 37 °C for 1 h. The reaction was stopped by 5 mM EDTA in PBS. The cells were lysed using 100 μl of 0.1% (w/v) sodium deoxycholate in PBS with 5 mM EDTA. The wells were blocked with 3% (w/v) BSA followed by incubation with Extravidin-peroxidase (1:5000). Incorporated biotinylated cadaverine was revealed using 3,3′,5,5′-tetramethylbenzidine. The resulting color was then read in an ELISA plate reader at 450 nm as above and represents the extracellular/cell surface TG2 activity. Assay linearity was demonstrated by a TG2 standard curve produced by applying purified guinea pig liver TG2 to wells containing no cells (supplemental Fig. 1C).

Detection of Extracellular Matrix-bound TG2 Antigen—Extracellular TG2 antigen was measured using a modified quantitative ELISA adapted from Achyuthan *et al.* (31) based on the ability of TG2 to adhere to fibronectin. 8×10^4 cells/well were plated into a fibronectin-coated 96-well plate. Cells were incubated in serum-free DMEM for 2 h at 37 °C and lysed with 0.1% deoxycholate in 5 mM EDTA. The remaining fibronectin layer containing TG2 was blocked with 3% BSA followed by incubation with anti-TG2 monoclonal antibody (cub7402, Abcam; 1:500) at 4 °C overnight. After a 0.1% Tween 20 wash, the wells were incubated with HRP-conjugated goat anti-mouse IgG (Dako; 1:1000) at 37 °C for 1 h. The color was revealed by 3,3′,5,5′-tetramethylbenzidine and read at 450 nm and represents the extracellular/cell surface TG2 antigen. Assay linearity and range were shown using a standard curve generated by the addition of recombinant human TG2 to wells containing no cells (supplemental Fig. 1D).

Fibronectin Knockdown by siRNA—The cells were cotransfected with 5 μg of DNA with 300 nM nonsense siRNA or anti-fibronectin 1 siRNA (Applied Biosystems) with TG2 cDNA using the Amaxa Nucleofector. The TG activity of the cell lysate, extracellular TG activity, antigen, and TG activity in the culture medium were measured 48 h after transfection, and the knockdown of fibronectin in the cell lysate was determined by 5% SDS-PAGE in reducing buffer followed by Western blotting for fibronectin.

Tracking TG2 with FlAsH-EDT2 Reagent and Co-localization Analysis—To visualize TG2 transport, NRK-52E cells were grown on sterilized microscope slide coverslips and incubated with 2.5 μM FlAsH-EDT2 reagent (Invitrogen) or CellMask plasma membrane staining as required (C10046, Invitrogen). The coverslip was rinsed in PBS and fixed with 4% paraformaldehyde. For co-localization, dual immunofluorescence staining was performed using the following antibodies at a 1:300 dilution: monoclonal anti-human collagen IV (C1926, Sigma), rabbit polyclonal human calnexin (endoplasmic reticulum) (C4731, Sigma), monoclonal anti-Golgi 58K protein (G2404, Sigma), and monoclonal anti-LAMP-2 (lysosomes) (SAB1402250, Sigma). Secondary antibodies were polyclonal anti-rabbit IgG-TRITC (T5268, Sigma) and anti-mouse IgG-TRITC at 1:500 (T5393, Sigma). Images were acquired on an Olympus BX-61 microscope using Cell-F software. Where applicable, images were deconvolved using AutoQuant X2 (Media Cybernetics, Silver Spring, MD) and three-dimensionally rendered using Imaris (Bitplane AG, Zurich, Switzerland).

Site-directed Mutagenesis—The QuikChange Site-Directed Mutagenesis kit with *Pfu*Turbo polymerase (Stratagene) was used according to the manufacturer's instructions. The forward and reverse primers were designed as described previously (32). PCR was performed for 12 cycles for one point mutation and 18 cycles for two point mutations.

HaloTag Protein Measurements—HaloTag protein was measured by ELISA according to the manufacturer's instructions. Briefly, 50 μl of cell lysate or culture medium was plated into a 96-well plate and incubated at 37 °C for 1 h. After three washes with 1% BSA, anti-HaloTag polyclonal antibody (G9281, Promega; 1:500) was added to the well and incubated for 1 h at 37 °C. Following three washes with 1% BSA, anti-rabbit immunoglobulins/HRP (1:1000) were added and incubated for 1 h at 37 °C. The anti-HaloTag protein polyclonal antibody and anti-rabbit immunoglobulin/HRP binding was revealed by 3,3′,5,5′-tetramethylbenzidine and read at 450 nm.

Statistical Analysis—The results were presented as mean ± S.E. and analyzed using one-way analysis of variance followed by a Bonferroni post hoc test. A p value less than 0.05 was considered statistically significant.

RESULTS

We engineered five constructs expressing domain deletion mutants of TG2 (three-dimensional construct images are shown in supplemental Fig. 2): TG2 lacking the β-sandwich domain (−bsw), the β-barrel 2 domain (−b2), both β-barrel domains (−b1b2), the β-sandwich and β-barrel 2 domains (−bswb2), and the β-sandwich and β-barrel 1 and 2 domains leaving just the TG2 core domain (core). Each construct was transiently transfected in three different tubular epithelial cell lines (TECs) (OK, NRK-52E, and MDCK II), and the externalization of the mutated TG2 was quantified. The standard curve for each assay used in this study and TG2 and mutant TG2 load according to the different amount of vector transfected are shown in supplemental Fig. 1.

Deletion Analysis: Total TG2 Activity and Antigen Post-transfection—Western blotting for TG2 in cell lysates demonstrated comparable increases in TG2 with all constructs and confirmed that appropriately sized proteins were produced (Fig. 1, *A–C*). TG activity in the cell lysates (Fig. 1, *D–F*) also increased equally for all constructs within each cell line. This indicated comparable transfection efficiency and that all domain deletions retained TG activity. Subsequently, TG2 transport could be tracked using extracellular TG activity assays.

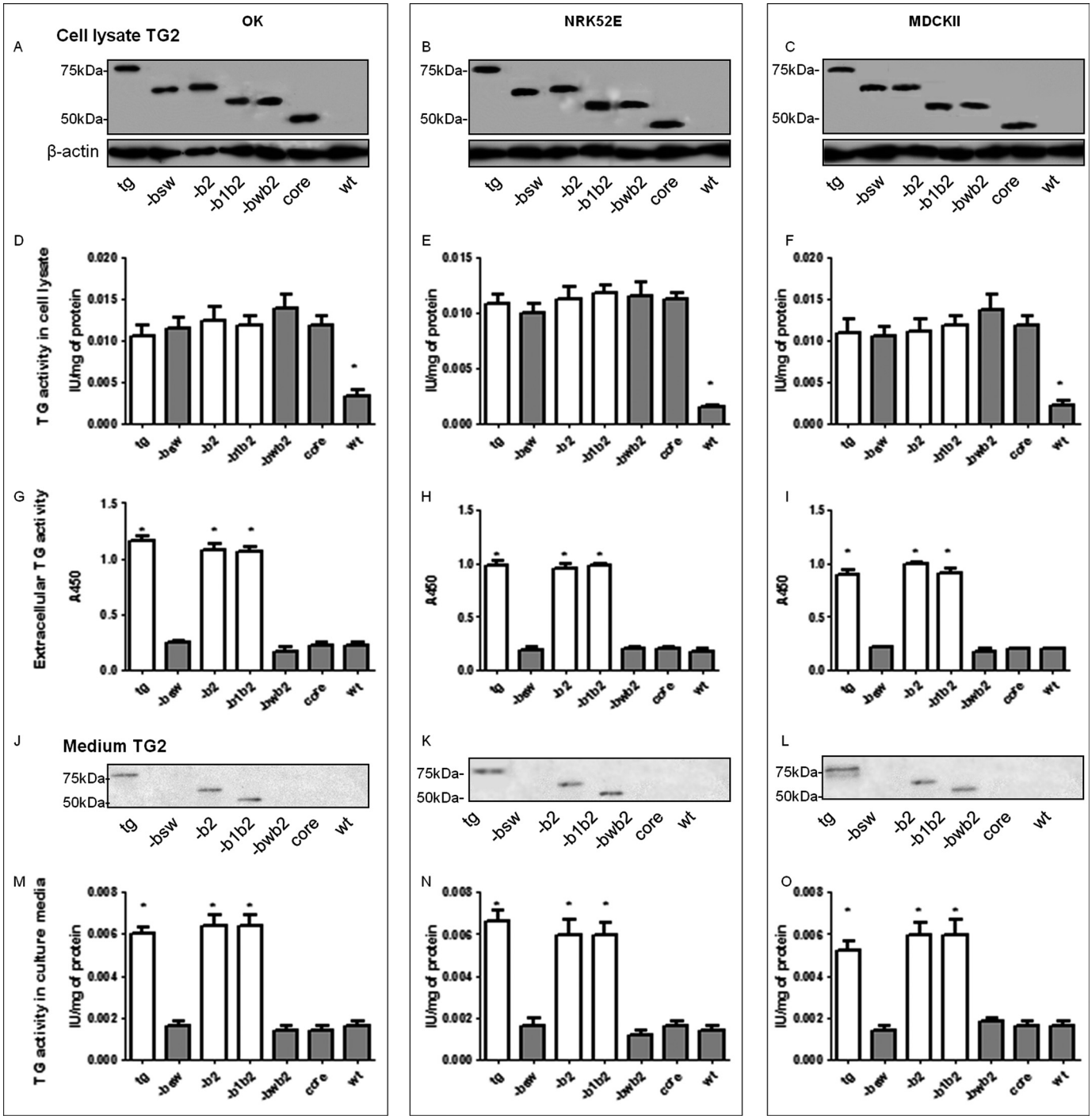

FIGURE 1. **Intra- and extracellular TG2 levels following domain deletion.** OK, NRK-52E, and MDCK II renal epithelial cells were transfected with the following constructs: 1) full-length TG2 (*tg*), 2) TG2 with β-sandwich domain deleted (−*bsw*), 3) TG2 with β-barrel 2 deleted (−*b2*), 4) TG2 with β-barrel 1 and β-barrel 2 domains deleted (−*b1b2*), 5) TG2 with both β-sandwich and β-barrel 2 domains deleted (−*bwb2*), and finally 6) TG2 catalytic core (*core*). The expression of TG2 is shown by Western blots in cell lysates 48 h post-transfection (*A–C*). Total TG activity in cell lysates (*D–F*), extracellular TG activity (*G–I*), Western blots for TG2 in culture medium (*J–L*), and TG activity in culture medium (*M–O*) were measured. *wt* indicates non-transfection control. Data represent mean values ± S.E.; $n = 5$; *, $p < 0.05$.

Deletion Analysis: Extracellular TG Activity and TG2 Antigen—Extracellular TG activity increased between 3- and 4-fold in all three cell lines transfected with full-length TG2 (Fig. 1, *G–I*), indicating that TG2 is readily trafficked to the extracellular environment after transfection in TECs. Similarly, cells transfected with TG2 cDNA with β-barrel 2 (−b2) and both β-barrel 1 and β-barrel 2 domains missing (−b1b2) had the same levels of extracellular TG activity as that of full-length TG2 in all three cell lines, suggesting that β-barrel domains played no role in TG2 externalization. Measurement of extracellular TG2 antigen in the media by Western blotting confirmed that constructs with β-barrel 2 (−b2) and both β-barrel 1 and β-barrel 2 domains missing (−b1b2) can be exported comparably with full-length TG2 (Fig. 1, *J–L*).

However, when cells were transfected with constructs in which the β-sandwich domain was missing (*i.e.* −bsw, −bwb2, and just core), extracellular TG activity was similar to that in cells that had not been transfected. This suggests that the transfected deletion mutant of TG2 is not being trafficked and that β-sandwich domain is crucial for TG2 transport.

As it is possible that removing a domain may not be affecting TG2 transport but simply its ability to localize to the cell surface or ECM (which the extracellular TG activity assay used predominantly measures), we repeated measurements of TG activity and antigen in the culture media to ensure that TG2 was not "floating" in the medium post-transport. In all three tubular epithelial cell lines, the TG2 fraction found in the medium mirrored measurements of extracellular TG activity both in terms of activity (Fig. 1, *M–O*) and antigen (Fig. 1, *J–L*), confirming that none of the constructs with β-sandwich domain missing can be detected in the medium.

Mutation Analysis—A previous report by Griffin and co-workers (33) on TG2 trafficking in transfected COS-7 cells had suggested that a fibronectin site encompassing the first 7 amino acids of the TG2 β-sandwich domain was crucial for TG2 export. To validate this in TECs, we deleted this site, transfected the construct, and assessed TG2 export as above. The construct (tg-7a) was transfected with efficiency equal to that of full-length TG2 (tg) and retained full activity (Fig. 2, *A* and *B*). However, the loss of the fibronectin binding site failed to prevent TG2 export (Fig. 2, *C–E*), suggesting that it is not important in TG2 export in tubular epithelial cells.

Examination of the literature revealed a second fibronectin binding site (^{88}WTATVVDQQDCTLSLQLTT^{106}) in the β-sandwich domain of TG2 (32), although this had not been implicated in TG2 trafficking. Subsequently, we introduced two point mutations (Asp^{94} and Asp^{97}) in this binding domain that had been shown previously to disable its binding to fibronectin (32). Constructs containing either one or both mutations were equally expressed (f1, f2, and f3) and had the same level of TG activity in the cell lysate as full-length TG2 (Fig. 3, *A–F*). However, single mutation of either Asp^{94} or Asp^{97} to Ala significantly decreased extracellular TG activity and antigen by 50% ($p < 0.05$), whereas two point mutation of Asp^{94} and Asp^{97} totally prevented TG2 export ($p < 0.05$) (Fig. 3, *G–I*) including TG2 in the media (Fig. 3, *J–O*). This indicates that this second fibronectin binding domain is critical for TG2 trafficking in TECs.

Effect of Deletion and Mutation of TG2 Export Sequence in Stably Transfected NRK-52E Cells—To confirm the results from deletion and mutation analyses, cloned, stably transfected NRK-52E cells containing full-length TG2, TG2 with β-sandwich domain missing (−bsw), and two point mutations (Asp^{94} and Asp^{97}; f3) were selected using blasticidin resistance. The expression of TG2 antigen (Fig. 4*A*) and activity (Fig. 4*B*) in cell lysates shows stable and comparable incorporation of all constructs. Cells expressing TG2 with the β-sandwich domain missing (−bsw) and two point mutations (f3) had no detectable TG2 antigen or activity outside the cell (Fig. 4, *C–E*), whereas cells expressing full-length TG2 did. These data are wholly consistent with the transient transfections used previously.

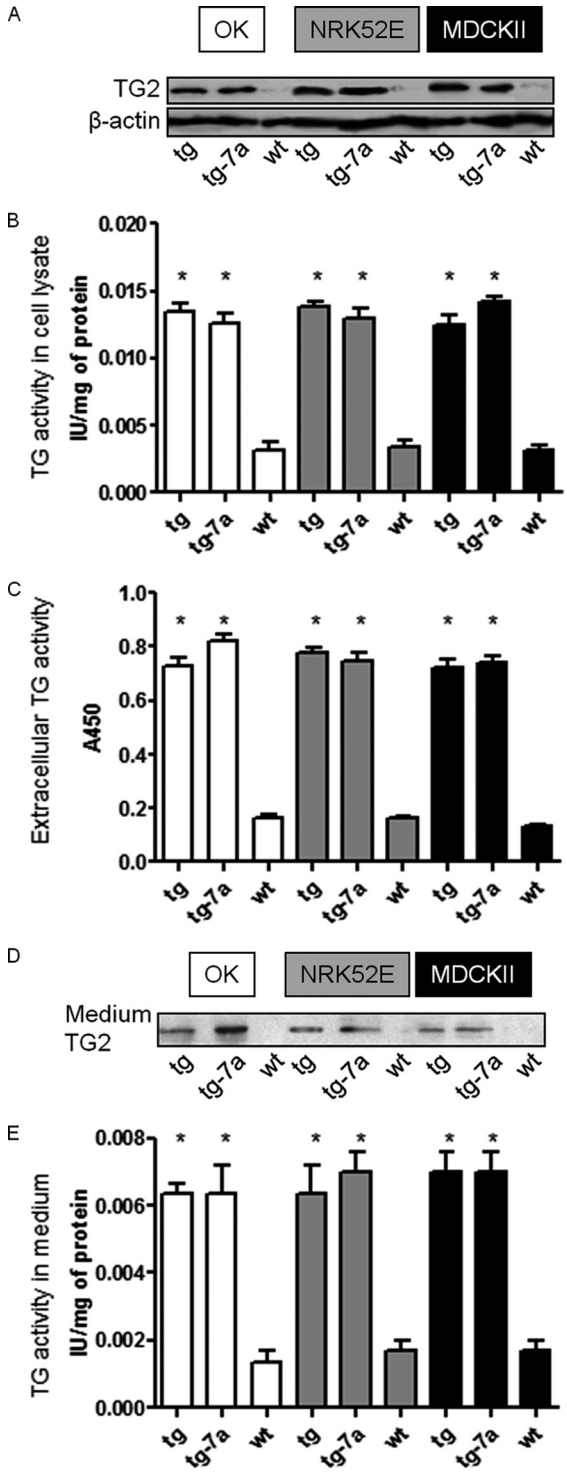

FIGURE 2. **Effect on TG2 export of removing amino acids 1–7 fibronectin binding site.** OK, NRK-52E, and MDCK II renal epithelial cells were transfected with full-length TG2 (*tg*) or mutant TG2 lacking the first 7 amino acids of β-sandwich domain that constitute a fibronectin binding site (*tg-7a*). Western blots for TG2 in cell lysates post-transfection are shown in *A*. Total TG activity in cell lysates (*B*), extracellular TG activity (*C*), Western blots for TG2 in culture medium (*D*), and TG activity in culture medium (*E*) were measured. *wt* indicates non-transfection control. Data represent mean values ± S.E; $n = 5$; *, $p < 0.05$.

TG2 Co-transport with Fibronectin—To assess whether TG2 is simply co-transported with fibronectin given that the crucial export sequence has been reported as a novel fibronectin binding site, we knocked down fibronectin using co-transfection of

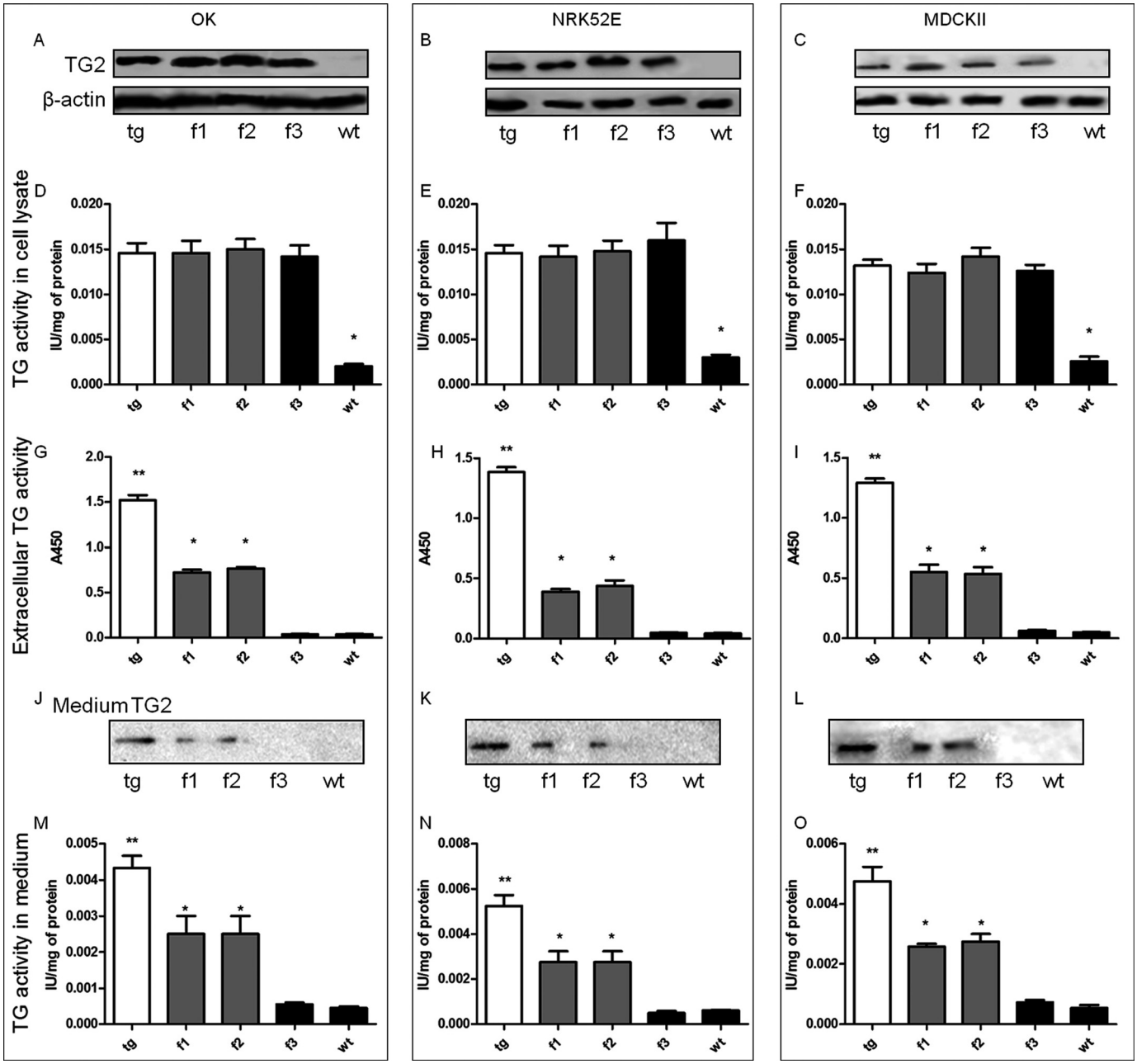

FIGURE 3. **Intra- and extracellular TG2 levels following point mutation.** OK, NRK-52E, and MDCK II renal epithelial cells were transfected with either 1) full-length TG2 (*tg*), 2) single point mutation of Asp^{94} to Ala (*f1*), 3) single point mutation of Asp^{97} to Ala (*f2*), or 4) a two-point mutation of TG2 at Asp^{94} and Asp^{97} to Ala (*f3*). TG2 expression is shown by Western blots for TG2 in cell lysates post-transfection (*A–C*). Total TG activity in cell lysates (*D–F*), extracellular TG activity (*G–I*), Western blots for TG2 in culture medium (*J–L*), and TG activity in culture medium (*M–O*) were measured. *wt* indicates non-transfection control. Data represent mean values ±S.E; $n = 5$; **, $p < 0.001$; *, $p < 0.05$.

anti-fibronectin siRNA with full-length TG2 (tg-f) in the cells. Fibronectin knockdown was confirmed by Western blot analysis (Fig. 5*A*). Volume densitometry measurements indicated that fibronectin was decreased by over 80% compared with fibronectin levels in cells co-transfected with nonsense siRNA and TG2 cDNA (tg-ns) in all three cell lines used. Measurements of extracellular TG activity, antigen, and TG activity in culture medium were identical irrespective of fibronectin knockdown (Fig. 5, *B–E*). Therefore, TG2 externalization appears to be independent of cell-secreted fibronectin, and thus TG2 is not co-transported with fibronectin.

Possible TG2 Externalization Pathways—Transfection with tetracysteine-tagged TG2 (nTC-Tag-DEST) allowed the use of FlAsH staining to color TG2 green under fluorescence so its movement could be tracked in the cell. This was used in combination with CellMask (red) to define the plasma membrane. TG2 in cells transfected with full-length TG2 and TG2 lacking the β-sandwich can clearly be seen inside the cell possibly in vesicles (Fig. 6, *B* and *C*, *white arrow*) with nothing visible in non-transfected cells (Fig. 6*A*). Following transfection of full-length TG2, green staining can also be seen between the cells clearly in the extracellular space (Fig. 6*B*, *yellow arrow*) as well

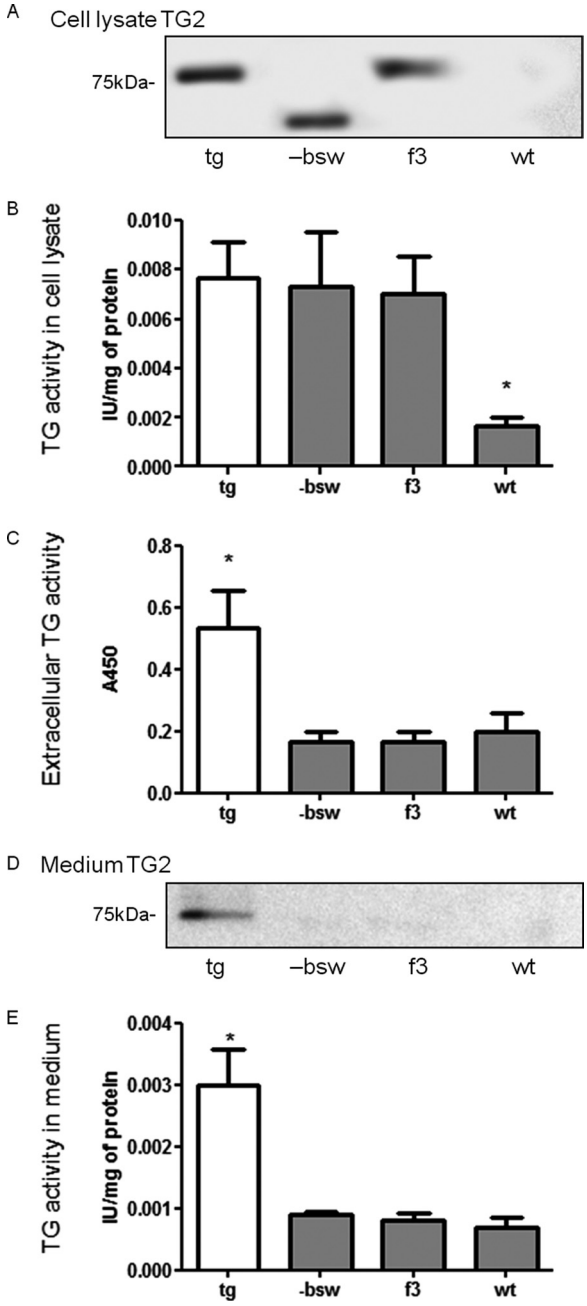

FIGURE 4. **Intra- and extracellular TG2 levels in NRK-52E cells stably transfected with mutant and full-length TG2.** NRK-52E renal epithelial cells were selected by blasticidin resistance after transfection with either wild type TG2 (*tg*), TG2 with β-sandwich domain deleted (−*bsw*), or a two-point mutation of TG2 at Asp^{94} and Asp^{97} to Ala (*f3*). Western blots for TG2 in cell lysates are shown in *A*, and TG2 in culture medium is shown in *B*. Total TG activity in cell lysate (*C*), extracellular TG activity (*D*), and TG activity in medium (*E*) were measured. *wt* indicates non-transfection control. *, $p < 0.05$.

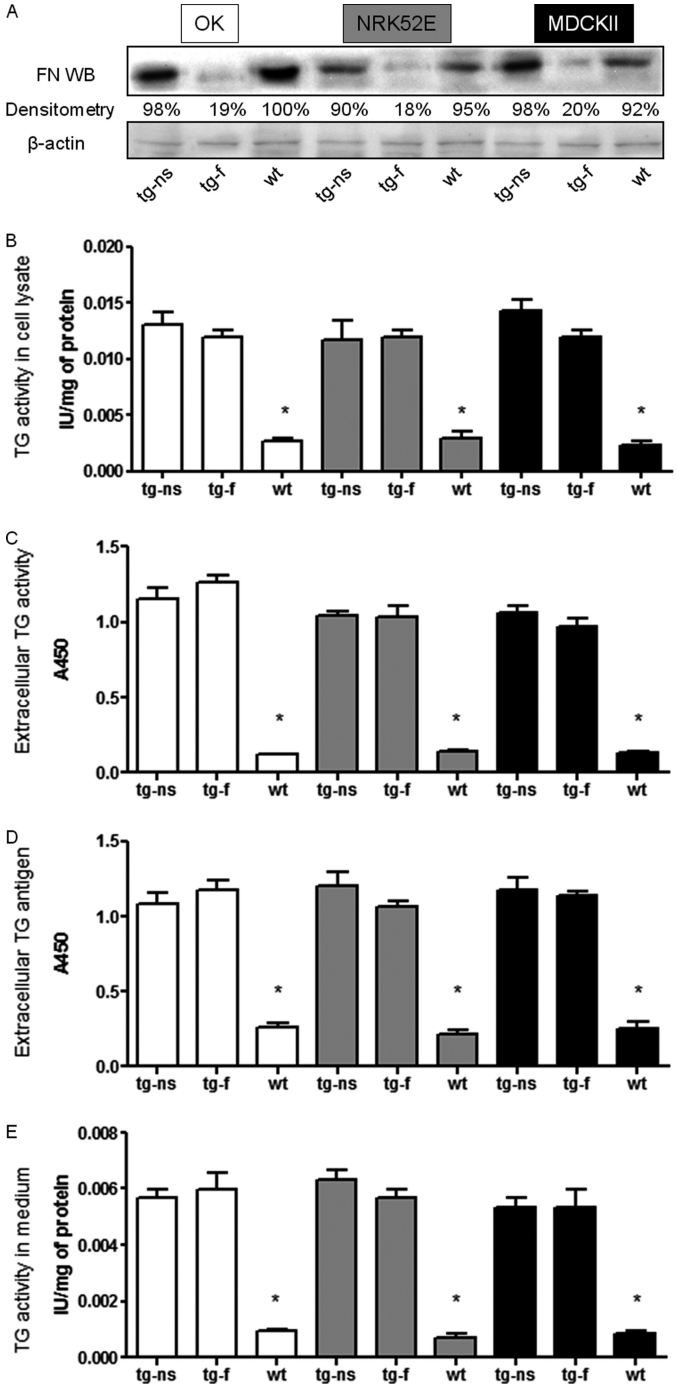

FIGURE 5. **Intra- and extracellular TG2 levels following fibronectin knockdown.** OK, NRK-52E, and MDCK II renal epithelial cells were co-transfected with TG2 plus either anti-fibronectin siRNA (*tg-f*) or nonsense siRNA (*tg-ns*). Western blots (*WB*) were used to show the basal fibronectin (*FN*) level in the cell lysate 48 h after transfection (*A*) with β-actin as a loading control. The values show volume density measurements as a percentage of the fibronectin knockdown. Total TG activity in cell lysates (*B*), extracellular TG activity (*C*), extracellular TG2 antigen (*D*), and TG activity in culture medium (*E*) were measured. *wt* indicates non-transfection control. $n = 5$; *, $p < 0.05$.

as in the plasma membrane, which appears *orange* with some intense *yellow spots* due to the co-localization of green and red fluorescence. Neither of these is seen following transfection with TG2 in which the β-sandwich domain was deleted. This imaging is consistent with the biochemical measurements of TG activity and antigen both in and out of the cell. To visualize the direction of TG2 transport, we used collagen IV (red) as a basolateral marker. Following deconvolution microscopy and three-dimensional rendering, TG2 (*green*) was not visible from above (Fig. 6*D*, *Apical view*) but was just visible at the bottom of the cells from the side (Fig. 6*E*, *Lateral view*), whereas basal views from underneath clearly show TG2 in the same plane as collagen IV (Fig. 6*F*). TG2 is therefore being exclusively exported to the basolateral side of the cells with the most abundant secretion of TG occurring directly under the nucleus.

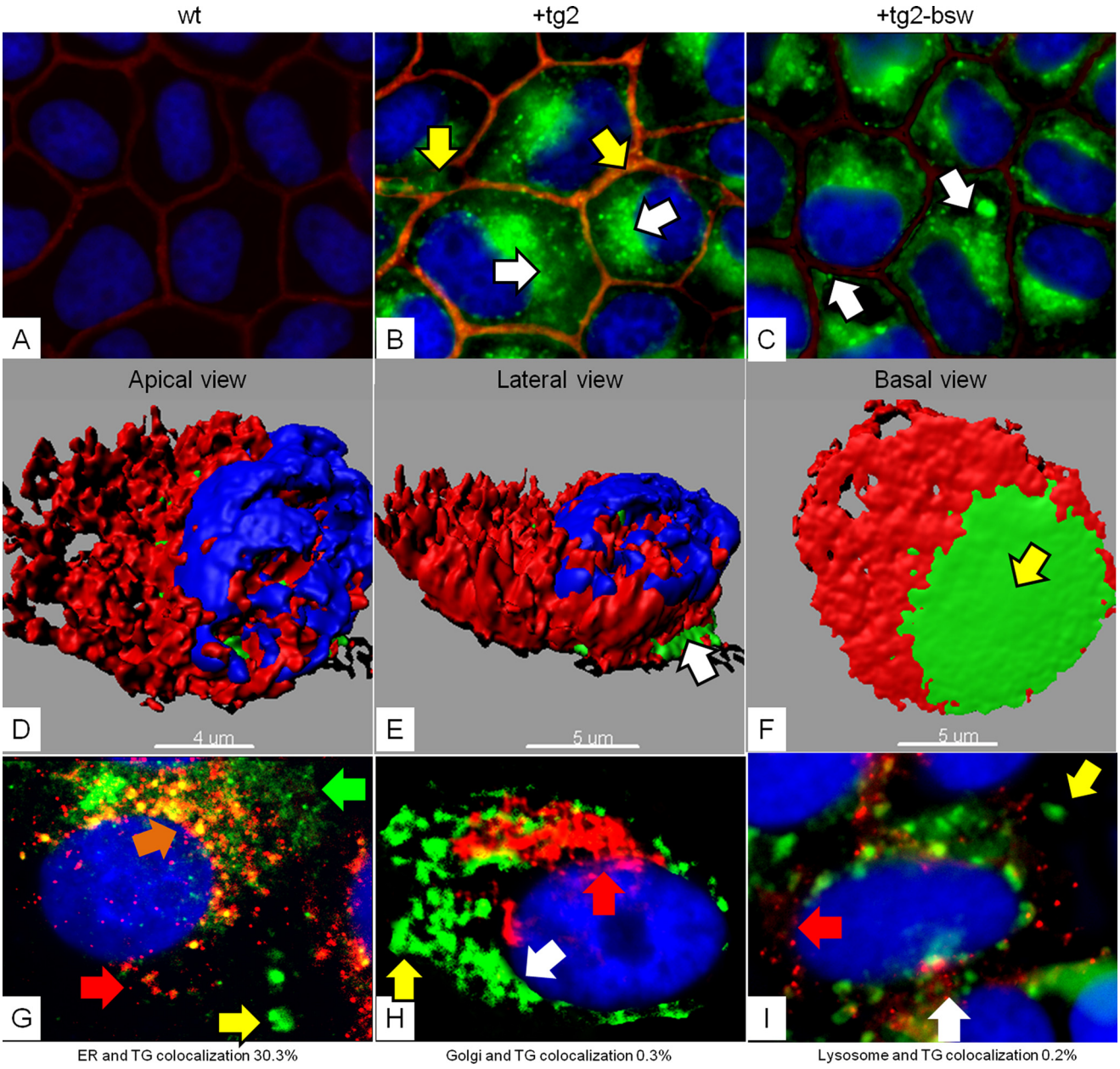

FIGURE 6. **Wild type and mutant TG2 fluorescence microscopy with cell organelle imaging.** Wild type NRK-52E cells (*A, wt*) were transfected with a tetracysteine Tag vector carrying either full length TG2 (*B, tg2*) or mutant TG2 with β-sandwich domain deleted (C, −*bsw*). Post-transfection cells were stained with FlAsH reagent coloring TG2 proteins (*green*) before the plasma membrane was stained using Cellmask plasma membrane reagent (*red*). Co-localization of TG2 and plasma membrane appears *orange*. *White arrows* indicate intracellular TG2 staining, and *yellow arrows* indicate extracellular TG2 staining. To determine the direction of TG2 export, TG2 transfected cells were again costained with FlAsH (*green*) and collagen IV (*red*). Three-dimensional images were generated and apical (*D*), side (*E*), and basal views (*F*) acquired. To assess colocalization with cell organelles, TG2 transfected cells were costained using organelles light (*red*) for ER. (*G*), Golgi apparatus (*H*), and lysosomes (*I*). Organelles are indicated by *red arrows*. In *G*, the *green arrow* shows peripheral TG2 (*green*) and the *orange arrow* shows TG2 around the cell nucleus that is colocalized with ER (*orange*). Cell nuclei are stained *blue* with DAPI.

Co-localization of TG2 (*yellow*; *orange arrow*) with endoplasmic reticulum (ER; *red arrow*) (Fig. 6*G*) showed that there was some co-localization of ER with TG2 around the cell nucleus (*orange arrow*); however, no peripheral TG2 (*green arrow*) was co-localized with ER, and no ER at all was seen near the periphery of these cells. Overall, 28% of the transfected TG2 was co-localized with the ER. There was only 0.3% co-localization of TG2 (*green*) with the Golgi apparatus (*red*) (Fig. 6*H*) and only 0.2% co-localization with lysosomes (*red*) (Fig. 6*I*), suggesting that TG2 is not externalized through Golgi- or lysosome-dependent routes.

Direction of TG2 Secretion—To confirm whether TG2 was being transported basolaterally (*i.e.* toward the tubular basement membrane) rather than apically (*i.e.* into the lumen), cells were grown in cell culture well inserts. Culture medium inside the insert represented apical secretion of TG2 and had a TG activity below the detection limit of the assay. In contrast, TG activity was 4 mIU/mg of protein in the culture medium outside the cell culture insert, indicating basolateral TG secretion to the basement membrane (Fig. 7).

Transport Motif—To assess whether the motif 88–106 itself is enough to target proteins for externalization in tubular epi-

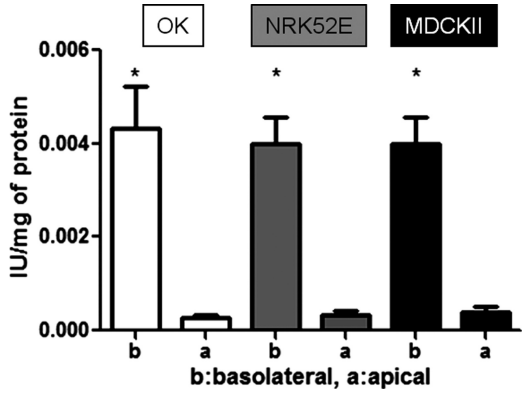

FIGURE 7. **TG2 is exported across basolateral membrane.** OK, NRK-52E, and MDCK II tubular epithelial cells were transfected with TG2 and plated in cell culture well inserts. TG activity of the culture medium below the insert (basolateral (*b*)) and within the insert (apical (*a*)) was measured in the culture medium. Date represent mean TG activity in units per milligram of protein ±S.E. *, $p < 0.05$; $n = 5$.

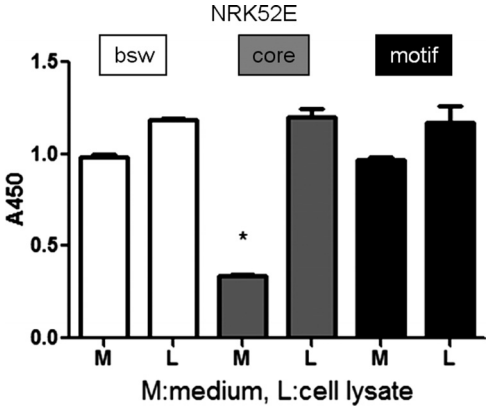

FIGURE 8. **Can TG2 export motif target other proteins for cell export?** The TG2 β-sandwich domain (*bsw*), TG2 core domain (*core*), and the TG2 export motif 88–106 (*motif*) were placed into the HaloTag vector pFC14K CMV. 48 h post-transfection the amount of HaloTag-labeled protein found in the culture medium and in cell lysates was assessed by anti-HaloTag polyclonal antibody. *L*, cell lysate; *M*, culture medium. Data represent mean HaloTag levels ±S.E. $n = 5$.

thelial cells, we inserted this motif, the β-sandwich domain, and the core domain (not transported) into a HaloTag vector and measured HaloTag protein levels in the cell lysate and culture medium (Fig. 8). The HaloTag ligand in the cell lysates was similar among all three constructs, indicating similar transfection efficiency and production. In contrast, when the HaloTag ligand was measured in culture medium, HaloTag linked to the TG2 export motif 88–106 and the TG2 β-sandwich domain was significantly higher than that linked to the core domain ($p < 0.05$) construct, suggesting that the motif 88–106 is capable of targeting proteins for externalization independently of the rest of the β-sandwich or TG2.

DISCUSSION

In this study, we found that the N-terminal β-sandwich domain, in particular the amino acid sequence 88–106 within the β-sandwich domain, is crucial for TG2 externalization in TECs. This finding is consistent across all three cell lines used with extracellular transglutaminase assessed using three different assays. Therefore, one can conclude this is not a cell line-specific effect or an artifact of a particular assay. As the identified sequence is not found in any other TG, targeting this sequence may provide a novel approach to interfere with the extracellular trafficking of TG2 seen in renal fibrosis.

In performing these studies, we initially expected that the cells transfected with TG2 mutants that were not exported would lead to higher TG levels in the cell lysate. However, practically no difference in total TG activity/antigen in the cell lysate was found despite the clear differences in TG2 outside the cell. These data initially appeared contradictory; however, by calculating the total amounts of TG2 in intracellular and extracellular compartments (supplemental Fig. 3) rather than per milligram of protein, it became evident that extracellular TG2 is only about 5% of the total TG in the cell lysate, and thus such small relative changes in intracellular TG2 levels would unlikely be detectable. However, when total intracellular and extracellular TG2 per well was calculated, two of the three cell lines did have higher mean intracellular values when transfected with non-exported TG2 constructs, although the differences were too small to reach statistical significance despite the multifold changes in extracellular TG2.

We chose to track TG2 by both antigen and activity routes to ensure robust data. Central to this was ensuring that the mutants did not have altered TG activity by measuring the activity in cell lysates. To confirm this, we also produced a TG2 core protein that displayed activity identical to wild type TG2, confirming that even with all other domains removed the TG2 core retained its activity.

Visualization of cells transfected with a non-exported mutant of TG2 showed some potential qualitative differences in addition to those shown in the figures that require further study. For example, when TG2 was not exported, the intracellular TG2 tended to accumulate in larger and more dense vesicle type structures closer to the nucleus. In addition, prior to confluence, cells transfected with non-exported mutants do not flatten to the same extent as those with wild type TG2 and thus appear to have a smaller diameter. This likely relates to the extracellular role of TG2 in cell adhesion, which is well known to cause this affect on morphology.

In the literature, four possible pathways have been proposed for unconventional protein secretion (Fig. 9*A*) (25). Proteins that are passed to the extracellular environment can be secreted through 1) lysosomes, 2) a direct molecular trap, 3) exosomes derived from multivesicular bodies, and 4) plasma membrane blebbing. Interleukin-1β is one of the unconventional secretary proteins linked to intracellular vesicles (34). The vesicles are positive for LAMP-1 and cathepsin D, which are both classical markers for lysosomes (35). In co-localization studies, TG2 was not co-localized with lysosomes, and therefore lysosome transport is unlikely to be involved in TG2 externalization. Increased sodium tolerance protein (Ist2) is another protein that passes through the plasma membrane without ER-to-Golgi transport (36). The newly synthesized Ist2 can be visualized by fluorescence microscopy, and it localized with ER at peripheral patches near the plasma membrane (37). We found that 30% of the ER stain was co-localized with TG2 (Fig. 6*G*); however, this was around the nucleus and consistent with TG2 synthesis at the ribosomes on the ER membrane, most likely in ER-bound polyribosomes. Neither ER (Fig. 9, *A*, *panel 3*) nor lysosomes

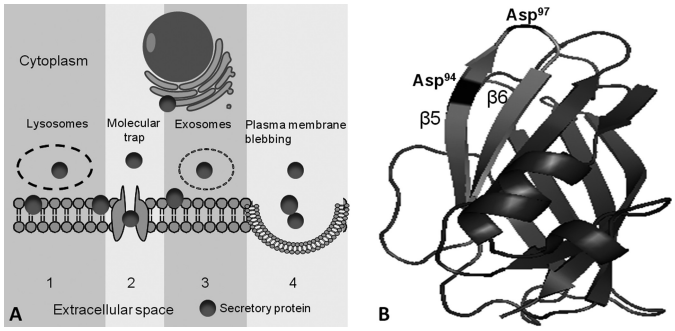

FIGURE 9. **Possible TG2 extracellular trafficking pathways and protein structure of β-sandwich domain.** *A*, schematic showing the known unconventional protein transmembrane transport routes. *Panel 1*, lysosome carrier route; *panel 2*, direct molecular trap mechanism; *panel 3*, exosomes derived from multivesicular bodies; *panel 4*, plasma membrane blebbing pathway. ●, indicates protein for export. *B*, protein structure of the TG2 β-sandwich domain showing the TG2 export motif (amino acids 88–106) lightly shaded with β5-strand and β6-strands labeled. *Black* indicates Asp^{94} and Asp^{97}.

(Fig. 9*A*, *panel 1*) were co-localized with TG2 in vesicles around the subplasma membrane area. In addition, a lack of TG2 was seen in plasma membrane blebs (Fig. 9*A*, *panel 4*) or exovesicles by fluorescence microscopy. TG2 externalization is mostly like linked to a direct molecular trap mechanism (Fig. 9*A*, *panel 2*).

Fibroblast growth factor (FGF-2) is a protein without a classical N-terminal signal peptide, its transmembrane transport is dependent on the cell surface heparan sulfate proteoglycans, and the transport involves a direct molecular trap on the cell surface (38). Recently, TG2 externalization has been related to the presence of cell surface heparan sulfate proteoglycans such as syndecan-4 (39) in primary skin fibroblasts as TG2 is known to bind heparin (40) and heparan sulfate (39). It remains to be established whether this pathway is relevant to TECs and whether amino acids 88–106 that make up the TG2 trafficking motif are critical for heparan sulfate binding (41). The accumulation of TG2 under the plasma membrane in the β-sandwich deletion and TG2 trafficking motif mutants would be consistent with such an export mechanism as would the identification of the TG2 export motif that is an absolute requirement for its export. Subsequently, identifying the proteins interacting with this export motif will be essential in determining the precise nature of the molecular trap mechanism and confirming this as a route for TG2 export.

Gaudry *et al.* (33) studied the interaction of fibronectin and TG2 using confocal microscopy co-localization studies. These experiments were performed in TG2-transfected COS-7 cells with cell surface TG2 determined using a β-galactosidase assay. They found that the first 7 amino acids in the N-terminal β-sandwich domain were important for cell surface TG2 with no binding to fibronectin if removed. In contrast, we report in TECs that the removal of the first 7 amino acids of the TG2 β-sandwich domain did not stop TG2 externalization. These discrepancies could simply mean that TECs handle TG2 export differently than fibroblasts. Of relevance, both Gaudry *et al.* (33) and we have identified perceived fibronectin binding sites as important in TG2 trafficking (even though fibronectin does not appear crucial for export). However, later work by Hang *et al.* (32) showed that the removal of amino acids 1–16 of the N-terminal β-sandwich domain did not affect TG2 binding to fibronectin. The motif, amino acids 88–106, we have identified as crucial for TG2 export is an interesting part of the β-sandwich forming a β5/β6 hairpin that is exposed on the surface of TG2. Asp^{94} and Asp^{97} are crucial for the β5/β6 hairpin to form (Fig. 9*B*), and subsequently the three-dimensional folding here is also critical TG2 for export. By adding a single mutation that would partially collapse the loop, we could partially prevent export, relating export to structure. Simply attaching this amino acid sequence to the C terminus of another protein (*e.g.* HaloTag) seems to target it for export, which confirms that it is the part of TG2 required for TG2 trafficking. There have been several hypotheses suggesting that TG2 could be co-transported with fibronectin; however, our 80% knockdown of fibronectin by siRNA had no effect on TG2 extracellular trafficking. This not only contradicts these hypotheses but also implies that the amino acid sequence 88–106 must have additional binding partners and/or properties. It is likely that this TG2 export motif can bind to other proteins that contain a fibronectin-like domain and that this can act as a transmembrane binding partner.

Using bioinformatics, we have confirmed that the sequence ^{88}WTATVVDQQDCTLSLQLTT^{106} is specific to TG2. Two very similar sequences were identified in two mammalian cell membrane proteins. The first is the P2X purinoceptor family (15 of 19 amino acids in common with TG2). These proteins are cell membrane ion channels and are activated by ATP (42–44). The other is Semaphorin/CD100 antigen (16 of 19 amino acids in common with TG2). This protein belongs to a large family of secreted and transmembrane proteins that function as repellent signals during axon guidance (45–47). Semaphorin in particular is interesting as it can be secreted and thus may have some common elements with TG2 export. However, little is known about Semaphorin export.

Perhaps unsurprisingly, we found that TG2 is transported basolaterally into what would be the tubular basement membrane *in vivo*. This finding is consistent with the function of TG2 in the cell adhesion process and its role in ECM deposition and stabilization (9) that become pathological in fibrosis (15). In regard to understanding the process of TG2 trafficking, it may be helpful if differences can be identified between the basal and apical membranes in terms of potential transmembrane proteins or channels (9).

In conclusion, TG2 is a protein without a leader sequence. Its transport to the extracellular environment is important in the development of renal fibrosis. This export mechanism is restricted to the basolateral membrane and wholly dependent on the amino acid sequence 88–106 within the N-terminal β-sandwich domain. Although this motif has fibronectin binding properties, export is independent of fibronectin. These findings are consistent across all tubular epithelial cells tested. Targeting this motif pharmacologically could "lock" TG2 in the cell, preventing its detrimental functions in chronic kidney disease.

REFERENCES

1. Verderio, E. A., Johnson, T., and Griffin, M. (2004) *Amino Acids* **26,** 387–404
2. Grenard, P., Bresson-Hadni, S., El Alaoui, S., Chevallier, M., Vuitton, D. A., and Ricard-Blum, S. (2001) *J. Hepatol.* **35,** 367–375

3. Griffin, M., Smith, L. L., and Wynne, J. (1979) *Br. J. Exp. Pathol.* **60,** 653–661
4. Small, K., Feng, J. F., Lorenz, J., Donnelly, E. T., Yu, A., Im, M. J., Dorn, G. W., 2nd, and Liggett, S. B. (1999) *J. Biol. Chem.* **274,** 21291–21296
5. Johnson, T. S., El-Koraie, A. F., Skill, N. J., Baddour, N. M., El Nahas, A. M., Njloma, M., Adam, A. G., and Griffin, M. (2003) *J. Am. Soc. Nephrol.* **14,** 2052–2062
6. Auld, G. C., Ritchie, H., Robbie, L. A., and Booth, N. A. (2001) *Arterioscler. Thromb. Vasc. Biol.* **21,** 1689–1694
7. Mosher, D. F. (1984) *Mol. Cell. Biochem.* **58,** 63–68
8. Lorand, L., and Conrad, S. M. (1984) *Mol. Cell. Biochem.* **58,** 9–35
9. Fisher, M., Jones, R. A., Huang, L., Haylor, J. L., El Nahas, M., Griffin, M., and Johnson, T. S. (2009) *Matrix Biol.* **28,** 20–31
10. Johnson, T. S., Skill, N. J., El Nahas, A. M., Oldroyd, S. D., Thomas, G. L., Douthwaite, J. A., Haylor, J. L., and Griffin, M. (1999) *J. Am. Soc. Nephrol.* **10,** 2146–2157
11. Huang, L., Haylor, J. L., Fisher, M., Hau, Z., El Nahas, A. M., Griffin, M., and Johnson, T. S. (2010) *Nephrol. Dial. Transplant.* **25,** 3897–3910
12. Suto, N., Ikura, K., and Sasaki, R. (1993) *J. Biol. Chem.* **268,** 7469–7473
13. Kuncio, G. S., Tsyganskaya, M., Zhu, J., Liu, S. L., Nagy, L., Thomazy, V., Davies, P. J., and Zern, M. A. (1998) *Am. J. Physiol. Gastrointest. Liver Physiol.* **274,** G240–G245
14. Skill, N. J., Johnson, T. S., Coutts, I. G., Saint, R. E., Fisher, M., Huang, L., El Nahas, A. M., Collighan, R. J., and Griffin, M. (2004) *J. Biol. Chem.* **279,** 47754–47762
15. Johnson, T. S., Fisher, M., Haylor, J. L., Hau, Z., Skill, N. J., Jones, R., Saint, R., Coutts, I., Vickers, M. E., El Nahas, A. M., and Griffin, M. (2007) *J. Am. Soc. Nephrol* **18,** 3078–3088
16. Huang, L., Haylor, J. L., Hau, Z., Jones, R. A., Vickers, M. E., Wagner, B., Griffin, M., Saint, R. E., Coutts, I. G., El Nahas, A. M., and Johnson, T. S. (2009) *Kidney Int.* **76,** 383–394
17. Shweke, N., Boulos, N., Jouanneau, C., Vandermeersch, S., Melino, G., Dussaule, J. C., Chatziantoniou, C., Ronco, P., and Boffa, J. J. (2008) *Am. J. Pathol.* **173,** 631–642
18. Skill, N. J., Griffin, M., El Nahas, A. M., Sanai, T., Haylor, J. L., Fisher, M., Jamie, M. F., Mould, N. N., and Johnson, T. S. (2001) *Lab. Invest.* **81,** 705–716
19. Akimov, S. S., and Belkin, A. M. (2001) *J. Cell Sci.* **114,** 2989–3000
20. Belkin, A. M., Akimov, S. S., Zaritskaya, L. S., Ratnikov, B. I., Deryugina, E. I., and Strongin, A. Y. (2001) *J. Biol. Chem.* **276,** 18415–18422
21. Akimov, S. S., and Belkin, A. M. (2001) *Blood* **98,** 1567–1576
22. Lodish, H. F. (2007) *Molecular Cell Biology*, 6th Ed., W. H. Freeman, New York
23. Ichinose, A., and Davie, E. W. (1988) *Proc. Natl. Acad. Sci. U.S.A.* **85,** 5829–5833
24. Ichinose, A., Hendrickson, L. E., Fujikawa, K., and Davie, E. W. (1986) *Biochemistry* **25,** 6900–6906
25. Nickel, W. (2005) *Traffic* **6,** 607–614
26. Gentile, V., Saydak, M., Chiocca, E. A., Akande, O., Birckbichler, P. J., Lee, K. N., Stein, J. P., and Davies, P. J. (1991) *J. Biol. Chem.* **266,** 478–483
27. Malström, K., Stange, G., and Murer, H. (1987) *Biochim. Biophys. Acta* **902,** 269–277
28. de Larco, J. E., and Todaro, G. J. (1978) *J. Cell. Physiol.* **94,** 335–342
29. Trigwell, S. M., Lynch, P. T., Griffin, M., Hargreaves, A. J., and Bonner, P. L. (2004) *Anal. Biochem.* **330,** 164–166
30. Jones, R. A., Nicholas, B., Mian, S., Davies, P. J., and Griffin, M. (1997) *J. Cell Sci.* **110,** 2461–2472
31. Achyuthan, K. E., Goodell, R. J., Kennedye, J. R., Lee, K. N., Henley, A., Stiefer, J. R., and Birckbichler, P. J. (1995) *J. Immunol. Methods* **180,** 69–79
32. Hang, J., Zemskov, E. A., Lorand, L., and Belkin, A. M. (2005) *J. Biol. Chem.* **280,** 23675–23683
33. Gaudry, C. A., Verderio, E., Aeschlimann, D., Cox, A., Smith, C., and Griffin, M. (1999) *J. Biol. Chem.* **274,** 30707–30714
34. Rubartelli, A., Cozzolino, F., Talio, M., and Sitia, R. (1990) *EMBO J.* **9,** 1503–1510
35. Andrei, C., Dazzi, C., Lotti, L., Torrisi, M. R., Chimini, G., and Rubartelli, A. (1999) *Mol. Biol. Cell* **10,** 1463–1475
36. Jüschke, C., Ferring, D., Jansen, R. P., and Seedorf, M. (2004) *Curr. Biol.* **14,** 406–411
37. Jüschke, C., Wächter, A., Schwappach, B., and Seedorf, M. (2005) *J. Cell Biol.* **169,** 613–622
38. Zehe, C., Engling, A., Wegehingel, S., Schäfer, T., and Nickel, W. (2006) *Proc. Natl. Acad. Sci. U.S.A.* **103,** 15479–15484
39. Scarpellini, A., Germack, R., Lortat-Jacob, H., Muramatsu, T., Billett, E., Johnson, T., and Verderio, E. A. (2009) *J. Biol. Chem.* **284,** 18411–18423
40. Gambetti, S., Dondi, A., Cervellati, C., Squerzanti, M., Pansini, F. S., and Bergamini, C. M. (2005) *Biochimie* **87,** 551–555
41. Verderio, E., and Scarpellini, A. (2010) *ScientificWorldJournal* **10,** 1073–1077
42. James, G., and Butt, A. M. (2002) *Eur. J. Pharmacol.* **447,** 247–260
43. Bo, X., Zhang, Y., Nassar, M., Burnstock, G., and Schoepfer, R. (1995) *FEBS Lett.* **375,** 129–133
44. Bo, X., Simon, J., Burnstock, G., and Barnard, E. A. (1992) *J. Biol. Chem.* **267,** 17581–17587
45. Hall, K. T., Boumsell, L., Schultze, J. L., Boussiotis, V. A., Dorfman, D. M., Cardoso, A. A., Bensussan, A., Nadler, L. M., and Freeman, G. J. (1996) *Proc. Natl. Acad. Sci. U.S.A.* **93,** 11780–11785
46. Hérold, C., Bismuth, G., Bensussan, A., and Boumsell, L. (1995) *Int. Immunol.* **7,** 1–8
47. Bougeret, C., Mansur, I. G., Dastot, H., Schmid, M., Mahouy, G., Bensussan, A., and Boumsell, L. (1992) *J. Immunol.* **148,** 318–323